Soil Biology & Biochemistry 100 (2016) 160–174

Contents lists available at ScienceDirect

Soil Biology & Biochemistry

journal homepage: www.elsevier.com/locate/soilbio

Using litter chemistry controls on microbial processes to partition litter carbon fluxes with the Litter Decomposition and Leaching (LIDEL) model

Eleanor E. Campbell [a, *], William J. Parton [a], Jennifer L. Soong [a, 1], Keith Paustian [a, b], N. Thompson Hobbs [a, c], M. Francesca Cotrufo [a, b]

[a] Natural Resource Ecology Laboratory, Colorado State University, 1231 East Drive, Fort Collins, CO 80523, USA
[b] Dept. of Soil and Crop Sciences, Colorado State University, Fort Collins, CO 80523, USA
[c] Dept. of Ecosystem Science and Sustainability, Colorado State University, Fort Collins, CO 80523, USA

ARTICLE INFO

Article history:
Received 5 January 2016
Received in revised form
27 May 2016
Accepted 13 June 2016
Available online 23 June 2016

Keywords:
Litter decomposition model
Leaching model
Microbial carbon use efficiency
Hierarchical Bayesian modeling
Lignocellulose
Nitrogen

ABSTRACT

New understanding of the connection between dynamic microbial carbon use efficiency (CUE), litter decomposition products, and pathways of soil organic carbon (SOC) formation have not been fully integrated into current generalizable litter decomposition models. We developed a new approach, the Litter Decomposition and Leaching (LIDEL) model, that: 1) includes leaching and formation of dissolved organic carbon (DOC), important components of vertical C movement and SOC inputs into deeper soil layers, and 2) uses widely available litter chemistry data to drive the simulation of microbial processes that partition litter during decomposition, through affecting rates of CO_2 respiration *versus* formation of microbial biomass and microbial products. Two ecologically important but poorly understood processes explored in this analysis include 1) the relationship between litter nitrogen (N) availability and rates of microbial decay and assimilation, and 2) the efficiency of DOC generation from the decomposition and leaching of soluble-*versus* cellulose-dominated plant litter fractions. We tested multiple hypothesis-driven model formulations, and for each estimated initial conditions and parameters using hierarchical Bayesian approaches. We combined data from experimental results and literature review for five types of litter that vary by initial lignin and N content. Our analyses showed the LIDEL model formulations with a logistic N limitation curve gave better predictions than model formulations using a linear N limitation curve. Model formulations with higher DOC generation efficiency from the soluble litter pool yielded more variable predictions and parameter estimations (shown by consistently wider 95% Bayesian credible intervals), but may have better simulated large DOC leaching events in early decomposition. Our analyses highlight a need for targeted studies clarifying measures of soluble litter and the generation of DOC during early litter decomposition, as well as rates of microbial biomass turnover and the flux of soluble *versus* non-soluble microbial products. Overall, the LIDEL model provides a robust generalizable framework to express and test hypotheses connecting litter chemistry and dynamic microbial CUE with the generation of DOC and microbial products during litter decomposition.

1. Introduction

Plant litter decomposition plays a key role in global carbon (C) cycling by directly linking terrestrial and atmospheric C pools (Houghton, 2007). The dynamics of this linkage are driven by decomposer interactions with the physical characteristics and chemistry of litter, as well as with other biotic and abiotic factors (e.g. climate) through time. Litter decomposition processes partition litter C, rapidly returning some to the atmosphere as respired CO_2 while generating other types and quantities of decomposition products (Don and Kalbitz, 2005), that then move through varying pathways of soil organic matter (SOM) formation (Cotrufo et al.,

* Corresponding author. Natural Resource Ecology Laboratory, Colorado State University, Fort Collins, CO 80523-1499, USA.
E-mail address: nell.campbell@colostate.edu (E.E. Campbell).
[1] Present address: Research Group of Plant and Vegetation Ecology, Department of Biology, University of Antwerp, Universiteitsplein 1, 2610 Wilrijk, Belgium.

http://dx.doi.org/10.1016/j.soilbio.2016.06.007
0038-0717/

2015). Accurately representing the partitioning of litter C between atmospheric return *versus* inputs to SOM formation pathways in ecosystem and global C cycle models is necessary to bridge vegetation models, to anticipate specific ecosystem responses to climate change, and to predict the magnitude and direction of feedbacks that affect global C dynamics.

Litter decomposition occurs through three general processes: fragmentation, catabolism to CO_2, and leaching (Swift et al., 1979). These processes yield inputs to SOM formation pathways that vary in chemistry, degree of microbial processing, and SOM formation efficiency through time (Cotrufo et al., 2015). Microbial carbon use efficiency (CUE)—the quantity of microbial biomass generated per unit of substrate use (Lekkerkerk et al., 1990)—is an important factor in the partitioning of litter C during decomposition, through the process of catabolism to CO_2 *versus* the formation of microbial biomass and products. Evidence suggests microbial CUE is often variable during litter decomposition, depending on the decomposition environment, chemical characteristics of substrates being decomposed, and the physiological characteristics of microbes and microbial communities (Frey et al., 2013; Lekkerkerk et al., 1990; Manzoni et al., 2008; Paustian and Schnurer, 1987). However, many widely used models simulate microbial CUE as a static variable (e.g. CENTURY (Parton et al., 1988)). Evidence supports microbial products as an important contributor to SOM formation (Cotrufo et al., 2015; Miltner et al., 2011; Schmidt et al., 2011). Litter decomposition models that include variable microbial CUE more accurately reflect partitioning of decomposed litter C to CO_2 *versus* microbial materials (e.g. Ingwersen et al., 2008; Pagel et al., 2014).

Many current litter decomposition models are also generally based on litter mass loss and CO_2 flux (Adair et al., 2008; Manzoni et al., 2012). This approach does not consider the generation of dissolved organic matter (DOM) with leaching, which can make up 6–39% of litter decomposition products (Don and Kalbitz, 2005; Magill and Aber, 2000; Qualls et al., 1991; Soong et al., 2015), and can be an efficient contributor to SOM formation in early litter decomposition (Cotrufo et al., 2015; Haddix et al., 2016).

DOM generated with leaching from decomposing litter is a dynamic mixture of soluble plant and microbial material that varies in quantity and chemistry between litter types and through time. Furthermore, patterns of DOM generation from litter are often unrelated to the dynamics of litter mass loss (Don and Kalbitz, 2005; Klotzbücher et al., 2011). The need to accurately reflect DOM dynamics and connections to SOM stabilization in ecosystem models has been recognized (Schmidt et al., 2011; Stockmann et al., 2013), particularly with evidence for the importance of DOM inputs and movement in deep soil layers (Rumpel and Kögel-Knabner, 2010). Several models do simulate soil DOM movement with leaching (e.g. Ahrens et al., 2015; Braakhekke et al., 2013; Ota et al., 2013; Tipping et al., 2012). However, many of these models pay limited attention to controls on DOM generation with leaching from litter or the variations in patterns of DOM generation across litter types, instead often partitioning the DOM from bulk litter as a set (e.g. Ahrens et al., 2015) or fitted (e.g. Braakhekke et al., 2013; Ota et al., 2013) parameter. Furthermore, soluble and non-soluble microbial products have been shown to contribute to SOM formation with different efficiencies through time (Cotrufo et al., 2015; Haddix et al., 2016). Combining a dynamic model of DOM generation from litter with models of DOM movement in soils with leaching would support better evaluation of new hypotheses for the role of litter-derived DOM in SOM formation. It would also allow the integration of new understanding into more comprehensive models of OM cycling, either at a fine scale—e.g. within a specific soil profile—or more generally in global biogeochemical processes.

A litter decomposition model that integrates a) the generation of DOM with leaching, b) variable microbial CUE and c) separate pathways for the movement of soluble and non-soluble microbial material with the turnover of microbial biomass generated from litter OM would incorporate this new understanding of litter C partitioning during decomposition. However, models of SOM dynamics must confront the fundamental tradeoffs between realism, precision, and generality (Levins, 1966), in the context of extremes in scale and heterogeneity (microsite to global, spatial, temporal), as well an evolving understanding of the connection between measured values and the biological, chemical, and physical factors driving SOM dynamics (Elliott et al., 1996; Simpson and Simpson, 2012; Stockmann et al., 2013). While some SOM modeling approaches are more widespread than others, no single modeling approach has emerged with universally superior performance (Campbell and Paustian, 2015). Several common modeling approaches used for site-to globally-scaled analyses are increasingly criticized for an inability to reflect new hypotheses for microbial roles in SOM formation (e.g. CENTURY, (Schmidt et al., 2011)). There are ongoing efforts to connect microbial processes observed in fine-scale laboratory and field experiments with large-scale models of OM dynamics (Fujita et al., 2014; Wieder et al., 2013), as well as address challenges in modeling microbial feedbacks (Wang et al., 2014). However, many uncertainties remain, and robust datasets to drive and evaluate model behavior at larger scales are scarce (Xu et al., 2013). Therefore, while there are existing micro-scale models of litter decomposition that include DOM formation and variable microbial CUE (e.g. Ingwersen et al., 2008; Pagel et al., 2014), there remains a need for a model of litter decomposition that includes these components, but with a more generalizable structure—e.g., generalizing microbial controls on litter C partitioning during litter decomposition—as a step towards reconciling key large-scale drivers widely included in common SOM modeling approaches with new hypotheses for microbial roles in litter decomposition and SOM formation. To meet these needs, we propose the Litter Decomposition and Leaching (LIDEL) model to reflect key litter chemistry drivers of microbial processes and litter C partitioning during decomposition, resulting in the generation of litter C products that enter different pathways of SOM formation (Fig. 1).

Litter N and lignin contents are both commonly measured and widely recognized as important drivers of litter decomposition (Adair et al., 2008; Aerts, 1997; Manzoni et al., 2008; Moorhead et al., 2013; Sinsabaugh et al., 2013). The LIDEL model dynamically links litter N and lignin content to microbial CUE by integrating hypotheses proposed by Moorhead et al. (2013) and Sinsabaugh et al. (2013). The LIDEL model also dynamically links litter N and lignin control on litter decomposition processes with the generation of plant- and microbially-derived DOC with leaching. Experimental data on litter C partitioning with leaching across these litter chemistries are extremely limited. Therefore, an experiment was designed to develop and test this aspect of the model. Details on the experiment are presented in Soong et al. (2015). With the LIDEL model, we look to simulate the partitioning of litter C with decomposition into C products that connect to new understanding of SOM formation pathways, as driven by key litter chemistry impacts on microbial processes, (i.e. being respired as CO_2 *versus* forming non-soluble microbial products or DOC), with a generalized structure that can be driven by broadly available litter chemistry data (Fig. 1).

There are a variety of established methods to integrate data with state-space models of C dynamics, in order to develop model structure, optimize model parameters and/or evaluate uncertainty in model performance (Del Grosso et al., 2010; Ogle et al., 2010, 2007). However, these analyses are often not satisfactory in accounting for multiple types of measurement data, accommodating different types of measurement and model uncertainty, or

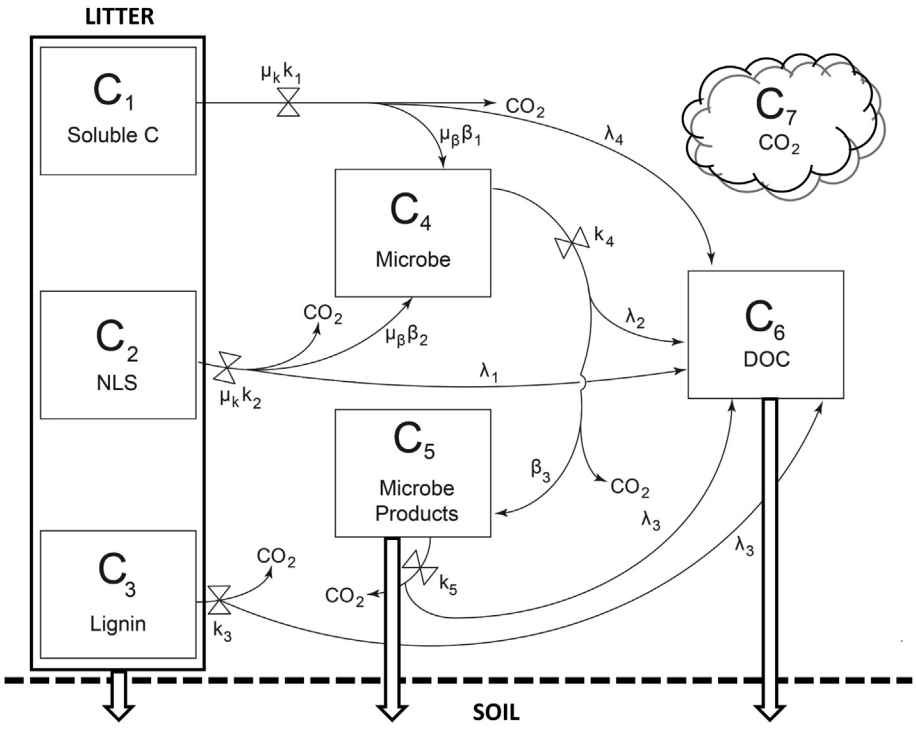

Fig. 1. Schematic showing the soluble (C_1), non-lignin structural (C_2, referred to as 'holocellulose' in text), lignin (C_3), microbial biomass (C_4), microbe products (C_5), dissolved organic carbon (DOC; C_6), and CO_2 (C_7) pools within the LIDEL model, in addition to the fluxes that connect model pools and the parameters that control the rates of these fluxes. The three litter pools (C_1, C_2, and C_3) generate microbial products (C_5) and DOC (C_6) as separate physical pools that, alongside remaining litter, can then enter soils and pathways for soil organic matter formation.

integrating these two components in time-series models. Bayesian methods for model-data integration provide a powerful approach to evaluate unknown model parameters and compare C cycling models (Tuomi et al., 2008), clarifying how measured data connect to ecological hypotheses (Hararuk and Luo, 2014). Bayesian methods can also help identify areas where data are needed or where additional data would help clarify the understanding of underlying dynamics (Ahrens et al., 2014; Braakhekke et al., 2014, 2013). Hierarchical Bayesian methods offer an approach to further parse sources of uncertainty and variation between process models (e.g. the LIDEL model), measured data, and model parameters (Berliner, 1996; Clark, 2007; Geremia et al., 2014). A hierarchical Bayesian approach has been used to successfully partition variability in soil respiration (Ogle and Pendall, 2015). In the hierarchical Bayesian framework it is also possible to separate model error from observation error if we use informative priors on error terms, for example if error in a specific measurement technique is well understood (Hobbs and Hooten, 2015).

The purpose of our paper is to present the LIDEL model as a generalizable litter decomposition model that can be used to express and test new hypotheses connecting litter chemistry controls on microbial processes, litter C partitioning, and the generation of inputs to key pathways of SOM formation. In this paper, we used data from Soong et al. (2015) and other literature to examine hypotheses for two ecologically important but poorly understood processes: 1) the relationship between litter N availability and rates of microbial decay and litter C assimilation, and 2) the efficiency of DOC generation from the decomposition and leaching of soluble-*versus* cellulose-dominated plant litter fractions. We applied hierarchical Bayesian methods for data-model integration, which allowed us to 1) evaluate four hypothesis-driven LIDEL model formulations, 2) estimate and compare parameter likelihoods under each model formulation, 3) clarify uncertainties in model dynamics given the available data and thus 4) identify specific datasets that would better inform subsequent development of model structure.

2. Material and methods

2.1. LIDEL model description

The LIDEL model (Fig. 1) is structured to model litter C partitioning via litter N and lignin controls on microbial litter decomposition processes, in order to dynamically simulate the generation of materials that enter different pathways of SOM formation. Litter is divided into three C fractions: water soluble, lignin, and non-lignin structural (abbreviated as NLS in Fig. 1). A similar fractionation approach separating plant litter into labile, lignin, and cellulose pools has been successfully applied in other models to include the impacts of microbial growth efficiency on C dynamics, yielding improved global simulations of soil C (Wieder et al., 2013). However, we used water-soluble litter instead of labile litter as a measure of potentially leachable litter material that can be released and transferred to the DOC pool through the influences of microbial processing and exposure to water.

We modeled lignin, similarly to Weider et al. (2013), in order to explicitly implement the Moorhead et al. (2013) hypotheses for lignin control on CUE, described below. The remaining litter material was estimated by difference and thus termed 'non-lignin structural'. However, we assumed that the 'non-lignin structural' fraction is dominated by cellulose and hemicellulose—termed holocellulose—and treated it as such when implementing Moorhead et al. (2013) hypotheses for lignin controls on decomposition. Here we refer to the 'non-lignin structural' pool using the more familiar term 'holocellulose', even though technically by our definition this pool also contains other non-soluble non-lignin material.

We modeled the movement of litter material into microbial biomass and then microbial products pools, with losses to DOC and CO_2, in order to incorporate dynamic microbial CUE impacts on the turnover of microbial biomass and the resulting generation of non-soluble microbial products *versus* DOC with leaching. It should be noted that in the LIDEL model lignin does not directly contribute to microbial biomass, but only decomposes to CO_2 and DOC. This simplifying assumption was drawn from the hypothesis that lignin is not energetically favorable for microbes to decompose, and is therefore largely decomposed in order to access holocellulose (Moorhead et al., 2013). It should also be noted that the LIDEL pool of microbial products only contained structural microbial material, as soluble microbial products from microbial biomass contribute to DOC with leaching (Fig. 1).

The LIDEL model consists of seven ordinary differential equations (Table 1, Eqs (1)–(7)) and runs on a daily time step. The initial conditions of the LIDEL model pools (referred to by τ subscripts) were determined by the measured fraction of initial litter material in the soluble, lignin, and DOC pools, with the remaining material allocated to the holocellulose pool (Table 1, Eqs (8)–(14)). Parameters β_1 and β_2—the maximum growth efficiencies (g microbial biomass per g decayed material) for microbial use respectively of water soluble and holocellulose litter—were set at values of 0.6 and 0.5, assuming the maximum CUE stipulated by Sinsabaugh et al. (2013) for soluble C and assuming a lower maximum for decomposition of holocellulose (Table 2). The remaining parameters were based on hypotheses described in the following sections.

2.1.1. Linking hypotheses for microbial CUE and litter decay

In the LIDEL model, we set a maximum CUE limit and a threshold for N effects on CUE (Moorhead et al., 2013; Sinsabaugh et al., 2013). Lignin affects litter decomposition, as well as microbial CUE, by limiting microbial access to usable plant material (i.e., holocellulose) (Herman et al., 2008; Manzoni et al., 2008; Moorhead et al., 2013; Sinsabaugh et al., 2013). We adapted these hypotheses to differentiate lignin and N limitations on decomposition and CUE, as based on the initial litter N content and a dynamic lignocellulose index (L_c, Table 2, Eq (15)).

Based on prior publications (Moorhead et al., 2013; Sinsabaugh et al., 2013) and DOC generation dynamics in the Soong et al. (2015) experiment, we hypothesized that the dynamics of water soluble and holocelluose pools are affected by both lignin and N. We assumed that the litter chemistry (i.e. either lignin protection of holocellulose, or N availability) exerting the greatest limitation at any given point in time during decomposition was, at that time point, controlling decay rates and microbial uptake of these pools (μ_k, Table 2, Eq (17) and μ_β, Table 2, Eq (19), respectively).

Moorhead et al. (2013) proposed that microbes do not decompose lignin when the lignocellulose index is less than 0.4, i.e. when holocellulose is highly available for microbial use. They further proposed a linear increase in rates of lignin decay accompanied by a linear decrease in rates of holocellulose decay when the lignocellulose index is between 0.4 and 0.7. Finally, they propose an equal decay rate of both pools when the lignocellulose index is greater than 0.7. We approximated these equations with continuous equivalents (ε_k, Table 2, Eq (18), Fig. 2A; ε_β, Table 2, Eq (20), Fig. 2B). We expressed the rate of lignin decay (k_3, in units of day^{-1}, Table 2, Eq (21)), based on the fitted parameter of the maximum rate of holocellulose decay (k_2). With this formulation, the rate of lignin decay will increase as L_c increases, until L_c=0.7, when the rate of lignin decay will equal the rate of cellulose decay if L_c is exerting the greatest limitation on decay rates (i.e. if the value of μ_k (Table 2, Eq (17)) = ε_k (Table 2, Eq (18))).

Non-soluble microbial products are hypothesized to be an important contributor to SOM formation (Cotrufo et al., 2013), but are difficult to measure (Preston et al., 2009), and their dynamics remain poorly understood. We assumed non-soluble microbial products decompose slowly and do not link this pool back to microbial biomass, making the simplifying assumption that this pool simulates microbial material that leaves the litter and enters the soil (Fig. 1). We expressed the rate of microbial products decay (k_5, in units of day^{-1}), for simplicity (i.e., without adding additional model parameters), as the same as the maximum possible rate of lignin decay (Table 2, Eq (22)).

Sinsabaugh et al. (2013) linked substrate N content to microbial CUE, providing evidence for a threshold for N availability above which N does not limit CUE. Based on this hypothesis, we proposed that above 3% N, either in litter or as available to microbes from external sources (e.g. soil, which we did not consider in this analysis), CUE and litter decomposition are unaffected by N availability. However, below that threshold we explored two mathematical expressions of N limitation (γ), 1) a logistic curve where N limitation on processes occurs strongly at a threshold value (Fig. 3, Table 2, Eq (16A)), *versus* 2) a linear curve where N limitation on processes occurs more gradually as N availability decreases (Fig. 3, Table 2, Eq (16B)).

2.1.2. Hypotheses from experimental data: DOC versus mass loss

Empirical relationships from Soong et al. (2015) and literature review were used to develop the remaining structure of the LIDEL model. In the Soong et al. (2015) experiment, five litter types were selected that exhibited a range of initial % N and initial lignocellulose indices (Table 3), in order to examine their relative impacts on the chemistry and quantity of DOC and CO_2 generation across a 365 day incubation. Each litter type was exposed to a microbial inoculum and allowed to decompose in absence of soil and without any additional N, with periodic leaching events that were more frequent in early stages of decomposition (initially every 1–3 days, then ca. weekly and later every 1–2 months). Leached DOC and CO_2 were measured at each leaching event. Litter mass loss was determined by destructive harvesting half of the samples at day 95 and the remaining half at the conclusion of the experiment on day 365 (for more details about the experiment see Soong et al. (2015)).

This experiment provided a unique dataset for explicitly evaluating the fractionation of DOC generation with leaching *versus* CO_2 through time, across litters that vary in their N and lignin chemistry. However, it should be noted that measures of leached DOC were taken at temporally variable intervals, even though the quantities of water leached at each experimental interval were equal. We accommodated this in our analysis by matching LIDEL modeled temporal intervals to each measurement temporal interval. Also, for simplicity the LIDEL model currently does not consider variable water exposure to generate DOC. Temporal intervals and quantities of water exposure both have the potential to impact the generation of DOC with leaching from decomposing litter, due to ongoing microbial processes that both generate and use potentially leachable material (Ingwersen et al., 2008; Tipping et al., 2012). We accommodated temporal variability in this analysis, but for simplicity assumed the impact of water volume was constant as this was a controlled variable in the Soong et al. (2015) experiment. However, the impact of water exposure that varies in quantity and timing is an area that will need further development to implement the LIDEL model in more general ecosystem models.

Given these assumptions, we hypothesized linearly declining relationships between the ratio of DOC *versus* litter mass loss (i.e. DOC/(DOC + CO_2)) as a function of initial litter % N and lignocellulose index, with the highest proportion of DOC generation at the lowest initial % N and lignocellulose index values. To develop this component of the LIDEL model, we first examined the predictive power of initial litter % N and lignocellulose index in estimating

Table 1
Mathematical representation of the LIDEL model, including differential equations for dynamics through time and equations to calculate initial conditions. All state variables are expressed as g C. Parameters contained in differential equations (Eqs 1–7) are defined in Table 2.

C pool	Equation	
C_1, *soluble litter C*	$\frac{dC_1}{dt} = \underbrace{-\mu_k k_1 C_1}_{\text{soluble litter decay}}$	(1)
C_2, *non − lignin structural (NLS, or 'holocellulose') litter C*	$\frac{dC_2}{dt} = \underbrace{-\mu_k k_2 C_2}_{\text{'holocellulose' litter decay}}$	(2)
C_3, *lignin litter C*	$\frac{dC_3}{dt} = \underbrace{-k_3 C_3}_{\text{lignin litter decay}}$	(3)
C_4, *microbial biomass C*	$\frac{dC_4}{dt} = \underbrace{-k_4 C_4}_{\text{microbial biomass decay}} + \underbrace{\mu_\beta \beta_2 (1-\lambda_1)\, \mu_k k_2 C_2}_{\text{microbial biomass from decayed 'holocellulose', after leaching}} + \underbrace{\mu_\beta \beta_1 (1-\lambda_4)\, \mu_k k_1 C_1}_{\text{microbial biomass from decayed soluble litter, after leaching}}$	(4)
C_5, *microbial products (non − soluble) C*	$\frac{dC_5}{dt} = \underbrace{-k_5 C_5}_{\text{microbial products decay}} + \underbrace{\beta_3 (1-\lambda_2) k_4 C_4}_{\text{microbial products from decayed microbial biomass}}$	(5)
C_6, *dissolved organic C*	$\frac{dC_6}{dt} = \underbrace{\lambda_1 \mu_k k_2 C_2}_{\text{leaching from decayed 'holocellulose' litter}} + \underbrace{\lambda_3 k_3 C_3}_{\text{leaching from decayed lignin litter}} + \underbrace{\lambda_2 k_4 C_4}_{\text{leaching from decayed microbial biomass}} + \underbrace{\lambda_3 k_5 C_5}_{\text{leaching from decayed microbial products}} + \underbrace{\lambda_4 \mu_k k_1 C_1}_{\text{leaching from decayed soluble litter}}$	(6)
C_7, $CO_2 - C$	$\frac{dC_7}{dt} = \underbrace{\left((1-\mu_\beta \beta_1)(1-\lambda_4)\right) \mu_k k_1 C_1}_{CO_2 \text{ from decayed soluble litter}} + \underbrace{\left((1-\mu_\beta \beta_2)(1-\lambda_1)\right) \mu_k k_2 C_2}_{CO_2 \text{ from decayed 'holocellulose' litter}} + \underbrace{(1-\lambda_3) k_3 C_3}_{CO_2 \text{ from decayed lignin litter}} + \underbrace{\left((1-\beta_3)(1-\lambda_2)\right) k_4 C_4}_{CO_2 \text{ from decayed microbial biomass}} + \underbrace{(1-\lambda_3) k_5 C_5}_{CO_2 \text{ from decayed microbial products}}$	(7)

With initial conditions (τ) by litter type (i) calculated as:

$$C_{1\tau i} = \left(C_{Ti}\, f_{s_i}\right) - \left(C_{Ti}\, f_{s_i}\, f_{DOC}\right) \quad (8)$$

$$C_{2\tau i} = C_{Ti} - \left(C_{Ti}\left(f_{s_i} + f_{LIG_i}\right)\right) \quad (9)$$

$$C_{3\tau i} = C_{Ti}\, f_{LIG_i} \quad (10)$$

$$C_{4\tau i} = 0 \quad (11)$$

$$C_{5\tau i} = 0 \quad (12)$$

$$C_{6\tau i} = C_{Ti}\, f_{s_i}\, f_{DOC} \quad (13)$$

$$C_{7\tau i} = 0 \quad (14)$$

Where, in initial condition equations:

- C_{Ti} = the total initial C mass of litter i
- f_{s_i} = the soluble fraction for a given litter i
- f_{DOC} = the fraction of soluble litter material that bypasses LIDEL microbial processes and is immediately released from plant litter into the DOC pool with leaching
- f_{LIG_i} = is the lignin fraction for a given litter i

Table 2
List of LIDEL model parameters, definitions, values of parameters or equations used to derive parameter values, and sources.

Parameter	Definition	Unit	Value	Equation reference	Source
Litter chemistry controls					
L_c	Lignocellulose index	–	lignin (C_3)/(lignin (C_3)+holocellulose (C_2))	(15)	Moorhead et al. (2013)
L_{cMax}	Maximum lignocellulose index value	–	0.51		Measured in Soong et al. (2015)
ϕ	Internally available initial litter % nitrogen	%	Table 3		Measured in Soong et al. (2015)
γ	Rate modifier based on nitrogen limitation	0–1 scaling	N Limitation Hypothesis 1 (logistic) $\frac{1}{1+e^{-N_{Max}(\phi-N_{mid})}}$	(16A)	Adapted from Sinsabaugh et al. (2013)
			N Limitation Hypothesis 2 (linear) for $N < N_{Max}$, $\gamma_{min} + \frac{1-\gamma_{min}}{N_{Max}}\ \phi$ for $N \geq N_{Max}$, 1	(16B)	
N_{Max}	Maximum initial litter % nitrogen for a nitrogen effect	%	3		Adapted from Sinsabaugh et al. (2013)
N_{mid}	Midpoint of the nitrogen limitation curve (N Limitation Hypothesis 1, logistic)	%	1.75		Value set to test hypotheses for N limitation
γ_{min}	Intercept determining the minimum value of γ (N Limitation Hypothesis 2, linear)	0–1 scaling	0.1		Value set to test hypotheses for N limitation
Selection of litter chemistry control on decomposition processes					
μ_k	Litter chemistry limitation on decay rate of water soluble litter C (C_1) and holocellulose litter C (C_2)	0–1 scaling	$\min(\gamma,\varepsilon_k)$	(17)	Analysis of data from Soong et al. (2015)
ε_k	Rate modifier for L_c-dependent limitation on decay	0–1 scaling	for $L_c < 0.7$: $exp^{-3.0*L_c}$ for $L_c \geq 0.7$: $exp^{-3.0*0.7}$	(18)	Adapted from Moorhead et al. (2013)
μ_β	Modifier for microbial biomass C (C_4) created from decayed water soluble (C_1) and holocellulose (C_2) litter	0–1 scaling	$\min(\gamma,\varepsilon_\beta)$	(19)	Analysis of data from Soong et al. (2015)
ε_β	Modifier for L_c-dependent limitation on microbial biomass C generation from decayed water soluble (C_1) and holocellulose (C_2) litter C	0–1 scaling	for $L_c < 0.7$: $1 - exp^{-0.7(\lvert L_c-0.7\rvert*10)}$ for $L_c \geq 0.7$: 0	(20)	Adapted from Moorhead et al. (2013)
Decay rates					
k_1	Maximum rate of water soluble litter C (C_1) decay	day^{-1}	Estimated		
k_2	Maximum rate of holocellulose litter C (C_2) decay	day^{-1}	Estimated		
k_3	Rate of lignin litter C (C_3) decay	day^{-1}	for $L_c < 0.7$: $k_2 \frac{0.2}{\left(1+\frac{200}{exp^{8.15L_c}}\right)}$ for $L_c \geq 0.7$: $k_2 e^{-3.0*0.7}$	(21)	Adapted from Moorhead et al. (2013)
k_4	Rate of microbe biomass C (C_4) decay	day^{-1}	Estimated		
k_5	Rate of microbial products C (C_5) decay	day^{-1}	$k_2 e^{-2.1}$	(22)	To minimize new parameters, set at maximum rate of lignin litter C decay (k_3)
DOC generation with leaching					
λ_1	DOC (C_6) generation with leaching from decay of holocellulose litter C (C_2)	g DOC (C_6) per g decayed holocellulose litter C (C_2)	$\min\left(\left(E_{HMax} - \frac{(E_{HMax}-E_{Hmin})}{L_{cMax}} * L_c\right), \left(E_{HMax} - \frac{(E_{HMax}-E_{Hmin})}{N_{Max}} * \phi\right)\right)$	(23)	Empirical relationships from Soong et al. (2015)
E_{Hmin}	Minimum leached DOC (C_6) from decayed holocellulose litter C (C_2)	g DOC (C_6) per g decayed holocellulose litter C (C_2)	DOC Generation Hypothesis 1 0.005 DOC Generation Hypothesis 2 0.001		Values set to test hypotheses for DOC generation efficiency
E_{HMax}	Maximum leached DOC (C_6) from decayed holocellulose litter C (C_2)	g DOC (C_6) per g decayed holocellulose litter C (C_2)	DOC Generation Hypothesis 1 0.15 DOC Generation Hypothesis 2 0.1		Values set to test hypotheses for DOC generation efficiency
λ_2	Generation of DOC (C_6) with leaching from decayed microbial biomass C (C_4)	g DOC (C_6) per g decayed microbial biomass C (C_4)	Estimated		
λ_3	Generation of DOC (C_6) with leaching from decayed microbial products C (C_5) and lignin litter C (C_3)	g DOC (C_6) per g decayed C	0.038		DOC generation from late stage alfalfa

(*continued on next page*)

Table 2 (*continued*)

Parameter	Definition	Unit	Value	Equation reference	Source
					decomposition in Soong et al. (2015)
λ_4	DOC generation (C_6) with leaching from decayed soluble litter C (C_1)	g DOC (C_6) per g decayed soluble litter C (C_1)	$\min\left(\left(E_{SMax} - \frac{(E_{SMax}-E_{Smin})*L_c}{L_{cMax}}\right), \left(E_{SMax} - \frac{(E_{SMax}-E_{Smin})*\phi}{N_{Max}}\right)\right)$	(24)	Empirical relationships from Soong et al. (2015)
E_{Smin}	Minimum leached DOC (C_6) from decayed soluble litter C (C_1)	g DOC (C_6) per g decayed soluble litter C (C_1)	DOC Generation Hypothesis 1 0.005 DOC Generation Hypothesis 2 0.1		Values set to test hypotheses for DOC generation efficiency
E_{SMax}	Maximum leached DOC (C_6) from decayed soluble litter C (C_1)	g DOC (C_6) per g decayed soluble litter C (C_1)	DOC Generation Hypothesis 1 0.15 DOC Generation Hypothesis 2 0.5		Values set to test hypotheses for DOC generation efficiency
Maximum growth efficiencies & generation of microbial products					
β_1	Maximum growth efficiency of microbial use of water soluble litter C (C_1)	g microbial biomass C (C_4) per g decayed soluble litter C (C_1)	0.6		Sinsabaugh et al. (2013)
β_2	Maximum growth efficiency of microbial use of holocellulose C (C_2)	g microbial biomass C (C_4) per g decayed holocellulose litter C (C_2)	0.5		Adapted from Sinsabaugh et al. (2013)
β_3	Generation of microbial products C (C_5) from microbial biomass C (C_4) decay	g microbial products C (C_5) per g decayed microbial biomass C (C_4)	Estimated		

total DOC generation with leaching, across the range of DOC *versus* litter mass loss measured in the Soong et al. (2015) experiment. We examined the predictive power of these relationships individually as well as by taking the minimum of the DOC *versus* mass loss predicted by each factor.

The generation of DOC with leaching is linked to the water soluble fraction of litter (Magill and Aber, 2000; Smolander and Kitunen, 2002). This is further supported by Soong et al. (2015) data that showed early DOC generation was strongly plant-derived, and strongly predicted by the hot water extractable fraction. We therefore assumed that early DOC generation was predominantly derived from the litter water soluble fraction. We hypothesized that DOC generated with leaching from both the water soluble (λ_4) and holocellulose (λ_1) litter fractions were similarly affected by initial litter % N and lignin (Table 2, Eq (24) and Eq (23), respectively).

We used these components of the LIDEL model to explore variation in DOC generation efficiency from leaching of the soluble *versus* holocellulose litter C pools, developing two formulations of the LIDEL model with respect to the maximum and minimum leached fractions from these pools. In one formulation these values were set equal to each other, at a minimum of 0.005 g DOC per g decayed soluble and holocellulose pools and a maximum of 0.15 g DOC per g decayed soluble and holocellulose pools. In the other formulation the soluble pool values were set higher than the holocellulose pool values, at 0.1 and 0.5 g DOC per g decayed soluble litter *versus* 0.001 and 0.1 g DOC per g decayed holocellulose. The latter approach assumed more efficient release of plant-derived DOC from decomposition of the soluble pool *versus* the holocellulose pool (Table 2, Eq (24) and Eq (23), respectively).

Finally, in the LIDEL model DOC was also generated with leaching from lignin, microbes, and microbial products C pools. The generation of soluble microbial products from microbial biomass turnover (λ_2) is not well understood and was a fitted parameter in this analysis. For the lignin and microbial products C pools, we assumed that only a small, constant portion of DOC was generated from ongoing decomposition processes (λ_3). We used measurements of DOC generation from late stage alfalfa decomposition (which decomposed quickly and had little mass at the end of the incubation (Soong et al., 2015)) to set this rate (Table 2).

2.2. Statistical approach

2.2.1. Data

Data used in this analysis included time series data from the laboratory litter decomposition experiment presented in Soong et al. (2015) and other data from previous studies (Adair et al., 2008; Parton et al., 2007) for the initial litter chemistry of the five litters; alfalfa (*Medicago sativa* L.), ash (*Fraxinus excelsior* L.), big bluestem (*Andropogon gerardii* Vitman), oak (*Quercus macrocarpa* Michx.) and pine (*Pinus ponderosa* Douglas ex P. Lawson & C. Lawson). To initialize the LIDEL model C pools, we used Soong et al. (2015) measurements of initial litter chemical fractions. The acid non-hydrolyzable residue of the acid detergent fiber digestion method (Van Soest and Wine, 1968) used by Soong et al. (2015) is a reasonable approximation of lignin at the initial phase of the experiment when the litters have not been exposed to microbial processing. However, the connection is less clear between the soluble C pool used in the LIDEL model and measurements from either hot water extraction (noted as HWE) or as the mass loss during neutral detergent fiber digestion (Soong et al., 2015). We used both of these measurements from Soong et al. (2015), supplemented with literature values across the five litters to more accurately reflect their variance (Adair et al., 2008; Parton et al.,

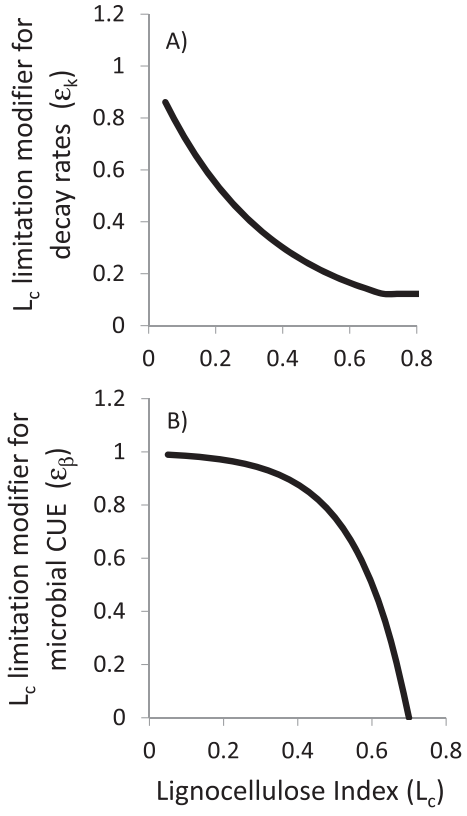

Fig. 2. Lignocellulose index (L_c) limitation modifier (y-axes) for soluble and holocellulose litter decay (A), and microbial carbon use efficiency (CUE) (B), by L_c values (x-axes). When L_c values are low, decay rates and microbial CUE are less limited (y-axis values closer to 1).

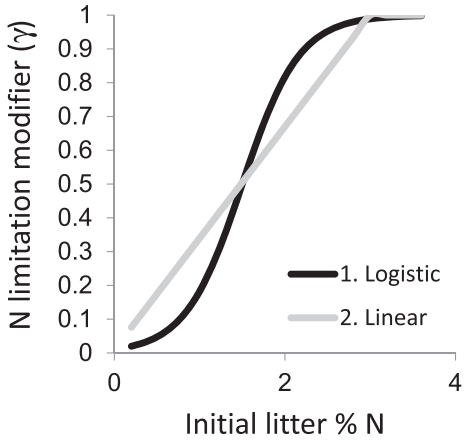

Fig. 3. Nitrogen (N) limitation modifier for microbial carbon use efficiency and rates of water soluble and holocellulose decay by initial litter percent nitrogen. Above the N limitation threshold (set at 3 percent N, drawn from Sinsabaugh et al. (2013)), N does not exert limitations (y-axis value = 1).

2007).

Conceptually, the initial value of the DOC pool in the LIDEL model represents the fraction of soluble litter C that is released with leaching alone, without interacting with microbial processes simulated in the LIDEL model. We made the assumption that the DOM characterized by high C:N observed in the first 10 days of the Soong et al. (2015) experiment was an approximation of this litter fraction, and used these data to set initial values for the LIDEL DOC pool. The initial holocellulose pool was assumed to comprise the remaining initial litter C after removal of the soluble and lignin components (Table 1, Eq (9)). Although microbial biomass was experimentally added to the litter with the inoculum in Soong et al. (2015), the initial LIDEL microbial biomass pool was set to 0 (Table 1, Eq (11)); the inoculum biomass was not generated from the litter C and was negligible on a mass basis compared to LIDEL C fluxes, particularly in early decomposition.

We also used CO_2, DOC, and total mass loss measurements from the 365 day incubation by Soong et al. (2015) to evaluate LIDEL temporal dynamics. Each time series measurement had three replicates for each litter. Full details on the data and their use to evaluate the LIDEL model are described in the supplemental material.

2.2.2. Hierarchical Bayesian analyses

Using the data described above, we estimated initial LIDEL model pools as well as five parameters that drive LIDEL temporal dynamics using a hierarchical Bayesian approach. The five parameters were the decay rates (day^{-1}) of the soluble (k_1), holocellulose (k_2), and microbial biomass pools (k_4), the generation of microbial products from microbial biomass (β_3, g microbial products per g decayed microbial biomass), and the generation of DOC from the decay of microbial biomass (λ_2, g DOC per g decayed microbial biomass). These parameters are important for the dynamics of litter decomposition through time as well as the generation of products from microbial processes. However, they are poorly understood in part due to the difficulty in measuring them experimentally.

The LIDEL model includes several equations where the minimum of two values drive model dynamics at a given point in time (Table 2, Eqs ((17), (19), (23) and (24)). The LIDEL model is therefore non-linear and cannot be solved analytically, requiring the use of an ordinary differential equations solver to resolve model dynamics using a daily time step.

We constructed two hierarchical Bayesian analyses. The first analysis estimated the initial conditions of the LIDEL model. The second analysis used the results of the first analysis as priors in the estimate of LIDEL temporal dynamics, repeated for each of the four LIDEL formulations (Table 4). This approach reduced the number of estimated parameters in the temporal dynamic analysis for each model formulation. Each temporal dynamic analysis used the posterior distributions of the initial condition analysis as priors to initialize LIDEL model pools on day 0.

To further simplify each temporal dynamic analysis, a subset of measured time points for DOC and CO_2 were used to estimate latent states and model parameters. The five main parameters of interest for each temporal dynamic analysis have single values across all

Table 3
Initial % N and lignocellulose index (L_c, or lignin/(lignin + holocellulose)) from Soong et al. (2015).

Litter	Mean initial %N	Mean initial lignocellulose index (L_c)
Alfalfa (*Medicago sativa*)	4.09	0.25
Ash (*Fraxinus excelsior*)	0.88	0.34
Bluestem (*Andropogon gerardii*)	0.48	0.20
Oak (*Quercus macrocarpa*)	1.32	0.46
Pine (*Pinus ponderosa*)	0.41	0.52

Table 4
Four LIDEL model formulations evaluated in this analysis, with all combinations of two shapes of N limitation curves and two approaches to DOC generation efficiency from microbial decomposition of soluble and holocellulose litter pools.

	Model 1	Model 2	Model 3	Model 4
Shape of N limitation curve:	Logistic	Logistic	Linear	Linear
DOC generation efficiency from decay of soluble and holocellulose litter pools:	DOC generated with equal efficiency	Soluble pool generates DOC more efficiently	DOC generated with equal efficiency	Soluble pool generates DOC more efficiently

litter types and all time points. Evaluating a subset of time points was considered an appropriate method to reduce computational complexity of the temporal dynamic Bayesian analysis by reducing the number of estimated values (by reducing the estimated latent states) while still informing the parameters of interest with time series measurements across the decomposition experiment. The subset of time points were selected to be representative of the 'early', 'middle' and 'late' stage decomposition dynamics discussed by Soong et al. (2015). The subset of time points included all measurements for all litter types on days 7, 15, 28, 64, 95, and 365. The remaining measurements were used for a non-exhaustive cross validation at each iteration of the MCMC, calculating the root mean square error (RMSE) for the model prediction of all measured time points excluded from the subset. Measurements of litter mass remaining were only taken at two time points, on day 95 and day 365. Therefore, all mass measurements were used in the temporal dynamic Bayesian analysis to estimate model parameters. RMSE results were an indication of model fit only for predicting out-of-sample DOC and CO_2 measurements.

Marginal posterior distributions of latent states and parameter marginal posterior distributions were approximated using random-walk Metropolis Hastings sampler in a Markov chain Monte Carlo (MCMC) algorithm. The analyses were written in R (R Core Team, 2014). We used the *lsoda* function in the R package *deSolve* as the ODE solver (Soetaert et al., 2010). Three chains of 100,000 iterations were accumulated for the initial conditions analysis. Inference was based on the final 50,000 iterations in the chains, discarding the first 50,000 iterations as the burn-in period. For the four LIDEL model formulations considered in each temporal dynamic analysis, three chains of 80,000 iterations each were simulated, with the first 40,000 iterations discarded as the burn-in period, with the exception of Model 3 where 100,000 iterations were simulated for each chain and the first 60,000 iterations discarded as burn-in. Individual chains were assessed visually for convergence using trace and marginal density plots, as well as using Geweke convergence diagnosis Z-scores (Geweke, 1992). The three chains for each analysis were then assessed for convergence using the Gelman-Rubin MCMC convergence diagnostic (Gelman and Rubin, 1992). Once the three chains passed convergence tests, summary statistics of model parameters were evaluated (mean and 95% Bayesian credible intervals). All convergence diagnoses and summary analyses were completed using the *coda* package in R (Plummer et al., 2006). Details for both the initial conditions and the temporal dynamic analyses, including the full expression for the posterior and joint distributions as well as MCMC algorithms, are described in the supplemental material.

3. Results

Our analyses of Soong et al. (2015) experimental data on DOC generation with leaching during litter decomposition showed that the empiric relationships between DOC generation with leaching and initial litter % N *versus* lignocellulose index had higher predictive power when using the minimum of the two factors, than when using either of these factors individually (predicted using minimum: $r^2 = 0.32$, slope = 0.62, intercept = 0.11; predicted using lignocellulose index: $r^2 = 0.15$, slope = 0.48, intercept = 0.11; predicted using initial litter % N: $r^2 = 0.11$, slope = 0.27, intercept = 0.13). This suggested litter N and lignin influence different mechanisms for DOC generation with leaching during decomposition. Predictions also had a higher r^2 as well as a slope closer to 1 and intercept closer to 0 when accounting for a higher proportion of DOC generation with leaching between early *versus* later decomposition (i.e. day 10–20 *versus* day 20–365), again using the minimum of predictions from initial litter % N and lignocellulose index (Fig. 4) (predicted using minimum: $r^2 = 0.86$, slope = 0.99, intercept = 0.018; predicted using lignocellulose index: $r^2 = 0.70$, slope = 0.90, intercept = 0.01; predicted using initial litter % N: $r^2 = 0.61$, slope = 0.70, intercept = 0.012). These results supported using the minimum of % initial litter N and lignocellulose index as empirical relationships to simulate dynamic DOC generation with leaching (all model formulations, Eqs (23) and (24)), as well as LIDEL model formulations simulating different efficiencies of DOC generation with leaching from the water soluble *versus* holocellulose litter pools (model formulations 2 and 4, Table 4).

Marginal posterior distributions of measurement variance for hot water extraction and mass-difference soluble fractions, as well as the posterior distributions of soluble fraction parameters by litter type (f_{s_i}, Table 1, Eqs. (8), (9) and (13)), are presented in Fig. 5. Although measurement variance was lower for soluble fractions estimated by mass-differences, as compared to those estimated by hot water extraction (Fig. 5A), neither measurement type varied consistently from the posterior distribution of litter soluble fractions (Fig. 5B). The posterior distribution of initial lignin fractions—informed by acid unhydrolyzable residue (AUR) data in the Soong et al. (2015) experiment—had a narrower width than the other litter fractions estimated in this analysis (Table 5), showing that the measured data more precisely informed the posterior distribution of litter lignin fractions.

The hierarchical Bayesian approach allowed litter fractionation

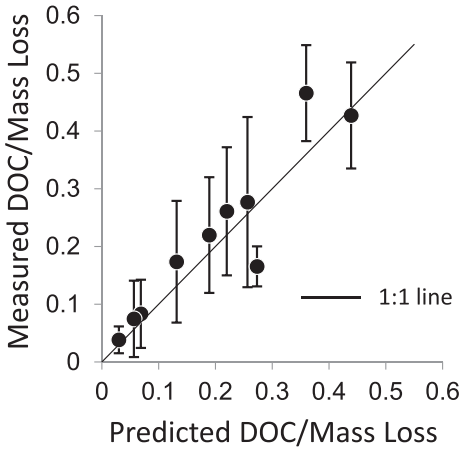

Fig. 4. Measured *versus* predicted dissolved organic carbon (DOC) generation per unit mass lost during decomposition, taking the minimum of the predicted fractionation based on percent initial litter nitrogen and initial lignocellulose index, for early and late-stage decomposition.

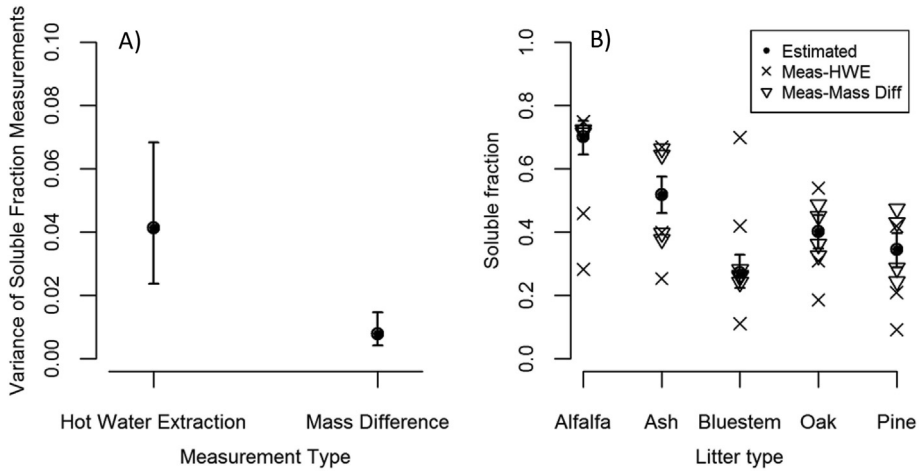

Fig. 5. Initial condition Bayesian analysis results, showing means (circular points) and 95% Bayesian credible intervals (lines) of estimated variance parameters for hot water extraction and mass-difference measurements of the litter soluble fractions (A), as well as the means (circular points) and 95% BCIs (lines) for final estimate of the soluble fraction parameters by litter type as compared to values using hot water extraction (x points) and by mass difference (triangular points) (B).

Table 5
Estimated parameters for fractions used to initialize LIDEL model pools, reporting mean and 95% Bayesian credible intervals (BCI) as well as credible interval widths. Narrower widths indicate a narrower range where, with 95% likelihood, the true value of each fraction is contained.

Fraction	Litter	Mean	95% BCI	95% BCI width
DOC (f_{DOC})	All	0.15	0.09–0.21	0.12
Soluble C (f_{S_i})	Alfalfa	0.70	0.65–0.75	0.11
	Ash	0.52	0.46–0.58	0.11
	Bluestem	0.27	0.22–0.33	0.11
	Oak	0.40	0.35–0.45	0.11
	Pine	0.35	0.29–0.40	0.11
Lignin C (f_{LIG_i})	Alfalfa	0.08	0.05–0.12	0.07
	Ash	0.15	0.11–0.18	0.08
	Bluestem	0.13	0.09–0.16	0.07
	Oak	0.27	0.23–0.31	0.08
	Pine	0.32	0.28–0.38	0.08

parameter variance and uncertainty, estimated in the initial conditions analysis, to be carried into the evaluation of LIDEL temporal dynamics. There were no clear trends in posterior distributions of parameter k_1 (rate of soluble litter pool decay, day^{-1}) across model formulations, although models 1, 2 and 4 had comparable posterior means, and in model 4 this parameter had a broader 95% Bayesian confidence interval (BCI) width (Table 6), showing its posterior distribution was less informed by the data. Estimates of k_2 (rate of holocellulose decay, day^{-1}) had narrower 95% BCI widths, with posterior distributions that were more informed by the data for all model formulations (Table 6). Microbial biomass turnover (k_4) had broad 95% BCI widths but suggested fast turnover, with all posterior distribution means exceeding 0.5 and with values that were closer to the upper range of the 95% BCI than the lower range (indicating a predominance of higher parameter values in the MCMC). The posterior distributions of microbial product generation from microbial biomass turnover (β_3) were very weakly informed by the data for all model formulations (Table 6). DOC generation with leaching from the decay of microbial biomass (λ_2) had narrower 95% BCI widths, with posterior means that were grouped by model formulations of N limitation curves (i.e. showing similar characteristics in models 1 & 2 (higher) *versus* models 3 & 4 (lower, Table 6)).

There was high variability in the posterior distribution of LIDEL model predictions of out-of-sample CO_2, without any clear trend by model formulation (Fig. 6, column 2). This is likely related to litter fractionation parameter variance (Table 5) carried into estimates of LIDEL model pool initial conditions, combined with the weakly informed parameters for microbial biomass turnover (k_4) and microbial product generation from microbial biomass turnover (β_3) (Table 6). CO_2 prediction variance for Model 4 (Fig. 6-4B) was exceptionally high compared to other model results, which may be due to poor N control of decayed material from the soluble litter pool (i.e. when DOC was generated with leaching more efficiently from the soluble litter pool, but N limitation was expressed using a

Table 6
Mean and 95% Bayesian credible intervals for the five parameters estimated in the temporal dynamic Bayesian analysis for each LIDEL model formulation.

Parameters	k_1- Soluble decay		k_2- Holocellulose decay		k_4- Microbial biomass decay		β_3- Microbial products (MP) from microbial biomass (MB) decay		λ_2- DOC with leaching from decayed microbial biomass (MB)	
Unit	(day^{-1})		(day^{-1})		(day^{-1})		(g MP g decayed MB^{-1})		(g DOC g decayed MB^{-1})	
Model	Mean	95% BCI (*width*)	Mean	95% BCI (*width*)	Mean	95% BCI (*width*)	Mean	95% BCI (*width*)	Mean	95% BCI (*width*)
1	0.24	0.13–0.50 (*0.37*)	0.0079	0.0016–0.016 (*0.0144*)	0.60	0.14–0.97 (*0.83*)	0.27	0.022–0.76 (*0.738*)	0.16	0.018–0.41 (*0.392*)
2	0.37	0.16–0.70 (*0.54*)	0.0090	0.0011–0.020 (*0.0189*)	0.57	0.11–0.97 (*0.86*)	0.33	0.028–0.79 (*0.762*)	0.19	0.022–0.42 (*0.398*)
3	0.095	0.038–0.20 (*0.162*)	0.0035	0.0015–0.0065 (*0.05*)	0.55	0.072–0.97 (*0.898*)	0.50	0.047–0.92 (*0.873*)	0.063	0.0091–0.23 (*0.221*)
4	0.28	0.071–0.93 (*0.859*)	0.0049	0.0018–0.012 (*0.0102*)	0.51	0.053–0.97 (*0.917*)	0.43	0.042–0.88 (*0.838*)	0.099	0.011–0.32 (*0.309*)

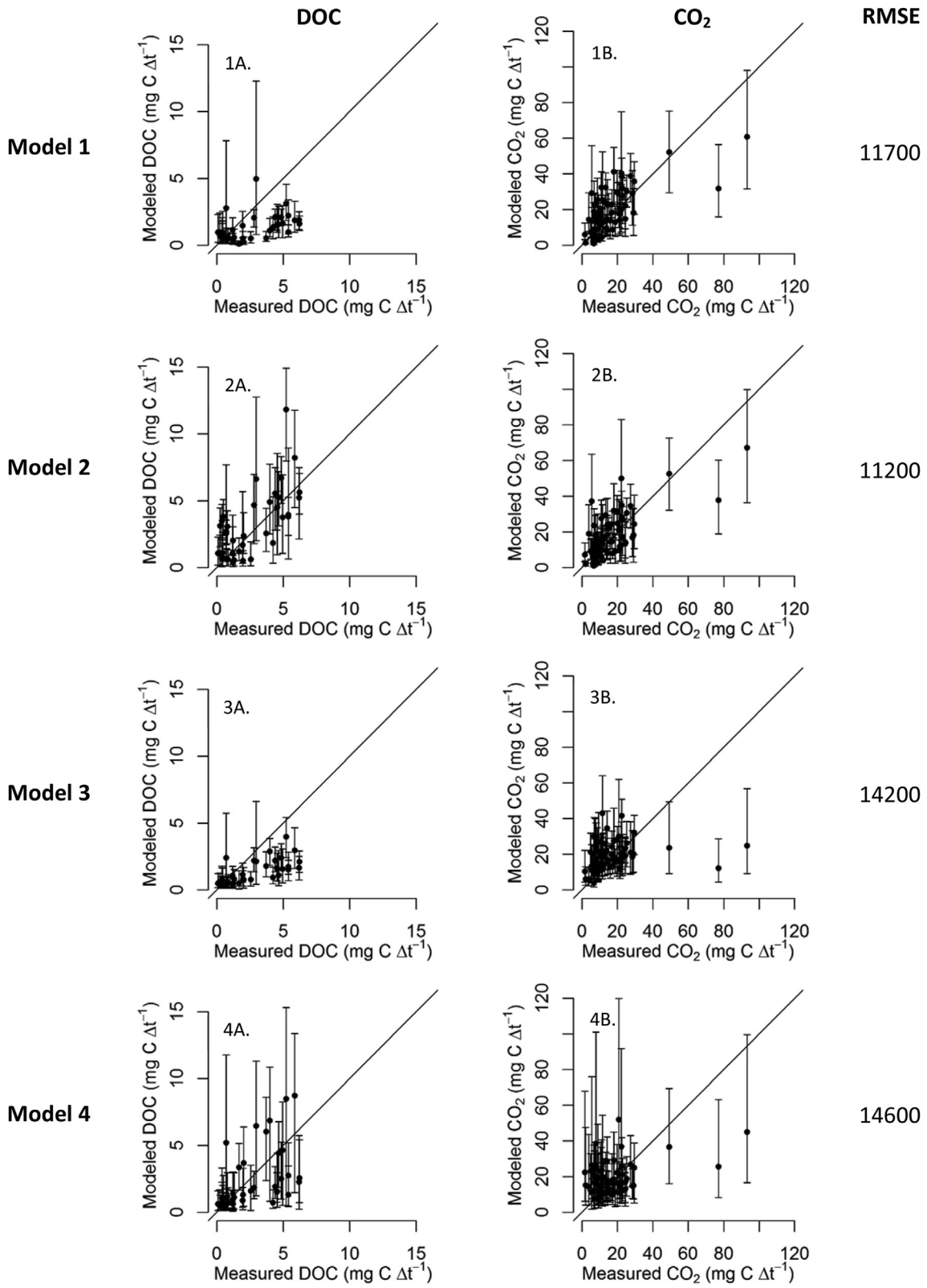

Fig. 6. Measured (x-axes), *versus* modeled (y-axes) LIDEL prediction of out-of-sample dissolved organic carbon (DOC, column 1) and CO_2 (column 2) measurements for the four LIDEL formulations, presenting posterior means (dark circles), 95% Bayesian credible intervals (vertical lines), and RMSEs (column 3). Diagonal lines indicate 1:1 relationships. LIDEL predictions of DOC are less variable with equal DOC generation efficiency from the soluble and holocellulose litter pools (narrower 95% BCIs, 1A and 3A), but these model formulations less consistently simulate high DOC values than the model formulations that have greater DOC generation efficiency from the soluble pool (higher number of 95% BCI widths for measured values > 4 mg C Δt^{-1} that intersect 1:1 line, 2A and 4A). For a majority of CO_2 predictions, the 95% BCIs intersect the 1:1 line, but their width indicates high variability in CO_2 predictions that is highest for Model 4 (4B). Model 2 showed the best fit overall, with the lowest RMSE.

linear curve (Table 4)). LIDEL predictions of out-of-sample DOC measurements were less variable for model formulations with equal DOC generation efficiency with leaching from the soluble and holocellulose pools (models 1 and 3, Fig. 6-1A and 3A), but were also less consistent predicting high measured DOC values (>4 mg C Δt^{-1}) than model formulations with greater DOC generation efficiency with leaching from the soluble litter pool (models 2 and 4, Fig. 6-2A and 4A). The Bayesian analysis of initial conditions yielded wide posterior distributions for the fractions of initial soluble and DOC pools (Table 5). This meant broad priors were used to inform the initial size of the soluble litter pool in the temporal dynamic Bayesian analysis. For all model formulations, the soluble LIDEL pool decomposed 1–2 orders of magnitude more quickly than the holocellulose pool (Table 6), making the soluble litter pool an important contributor to LIDEL dynamics particularly in early decomposition. The broad priors for the initial soluble pool size for each litter likely contributed strongly to variability in model estimates of DOC generation with leaching through time. Greater DOC generation efficiency with leaching from the soluble pool improved predictive accuracy in simulating high DOC generation, but also likely made the model more sensitive to uncertainty or variability in the size of the initial soluble litter pool. Cumulatively, models 3 and 4 had consistently higher RMSE values, showing overall poorer performance predicting out-of-sample DOC and CO_2 measurements compared to models 1 and 2 (Fig. 6).

The measured *versus* modeled comparison of in-sample mass loss time points also showed poorer LIDEL simulation of mass loss with models 3 and 4 *versus* models 1 and 2 (Fig. 7C and D *versus* 7A and B). These results, taken together with the results shown in Fig. 6, suggested a logistic curve (rather than a linear curve) is a better generalized representation of N limitation on microbial processes and the generation of DOC with leaching during litter decomposition.

4. Discussion

The LIDEL model incorporates key litter chemistry drivers of microbial processes and the explicit simulation of the generation of DOC with leaching *versus* structural microbial products during litter decomposition, partitioning litter C into materials shown to enter separate pathways of SOM formation (Cotrufo et al., 2015). This is an important new direction for the simulation of litter decomposition dynamics in SOM models. Our analyses supported the importance of the soluble litter fraction in both generating DOC and driving microbial dynamics, particularly during early litter decomposition. DOC leached from litter and persistent microbial products are both recognized as important contributors to SOM dynamics that are lacking in many SOM models (Rumpel and Kögel-Knabner, 2010; Schmidt et al., 2011). The LIDEL model provides a framework to dynamically simulate the source of these

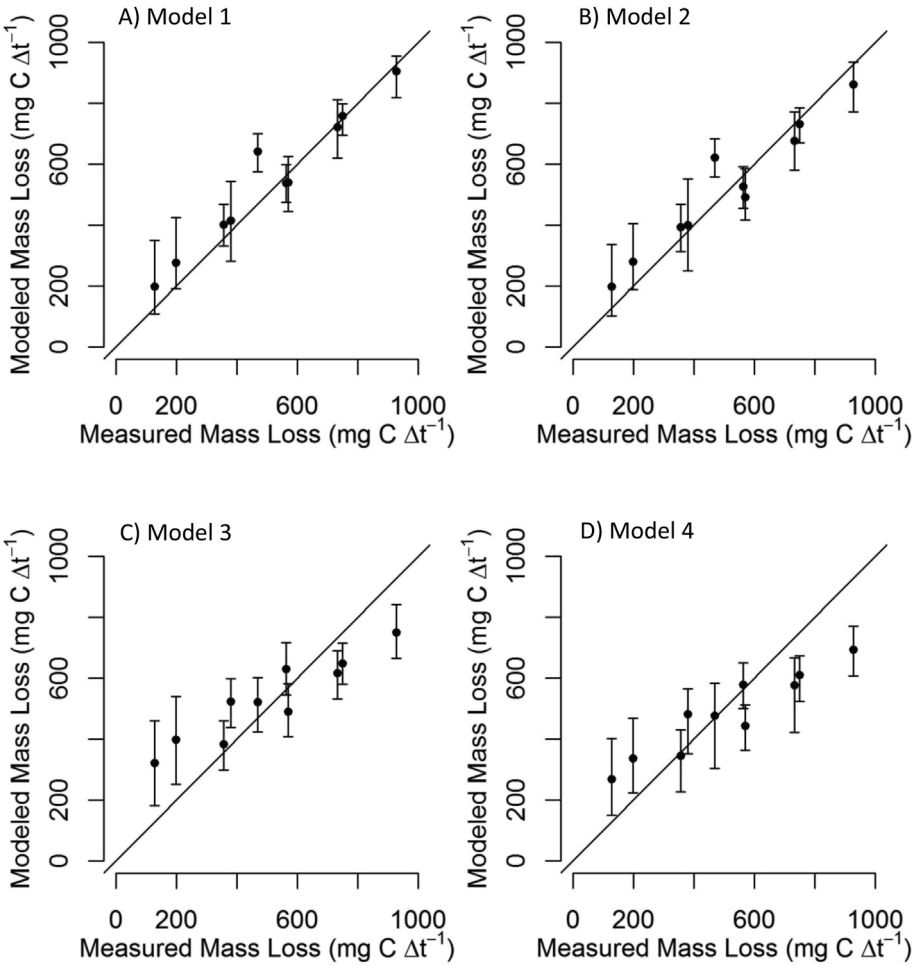

Fig. 7. Measured (x-axes), *versus* modeled (y-axes) LIDEL prediction of in-sample litter mass remaining, presenting posterior means (dark circles) and 95% Bayesian credible intervals for each LIDEL prediction (vertical lines). Diagonal lines indicate 1:1 relationships. The LIDEL model simulates mass loss more poorly with the linear nitrogen limitation curve (C and D) as compared to the logistic nitrogen limitation curve (A and B), shown by the higher number of BCI widths that fail to intersect the 1:1 line.

materials, an approach that would complement soil models simulating the dynamics of these materials as they move through the soil profile (Ahrens et al., 2015).

Our results showed that N limitation on microbial processes in the LIDEL model was better represented as occurring suddenly at a threshold (e.g. using a logistic curve), rather than gradually (e.g. using a linear curve) over increasing litter N availability. Accurately representing N control of microbial processes during litter decomposition is an important factor for modeling the connection between the litter OM inputs, microbial CUE, and soil C dynamics (Cotrufo et al., 2013; Sinsabaugh et al., 2013). It is also important for understanding ecosystem responses to direct and indirect human impacts, particularly in the context of managing soils for C sequestration (Prescott, 2010; Woo et al., 2014). In our analysis, one litter type (alfalfa) had a much higher N content than the others (Table 3). The LIDEL model could be further refined by evaluating a greater diversity of litters varying in N content, in order to estimate the location of the threshold as well as the magnitude of the effect once the threshold has been reached. In addition, our analysis did not consider external N availability; the litter incubation experiment from Soong et al. (2015) excluded soils, and only varied N by what was internally available in the different leaf litters. Calibrating the LIDEL model to dynamically simulate the effects of internal *versus* external N availability would expand the diversity of litter decomposition environments the model is able to simulate. Cumulatively, model 2—formulated using a logistic N limitation curve and a higher DOC generation efficiency with leaching from the soluble *versus* the holocellulose litter pool—showed the most promise for further developing the LIDEL model as a generalizable model of litter decomposition, accurately simulating litter mass loss (Fig. 7B) as well as high DOC fluxes using dynamic microbial CUE (Fig. 6-2A).

There are ongoing efforts to improve the representation of microbial dynamics in models of litter decomposition and SOM dynamics (Davidson et al., 2014; Moorhead and Sinsabaugh, 2006; Wieder et al., 2014, 2013). Many of these efforts are directed towards more explicit representation of microbial biomass, as well as mechanistic representation of microbial-driven processes (Stockmann et al., 2013; Treseder et al., 2012). However, there is the potential for increases in model complexity and unrealistic oscillatory behavior with the added feedback between explicit microbial biomass and decomposition dynamics (Wang et al., 2014). Data to drive and evaluate models with explicit microbial biomass and mechanisms are limited (Treseder et al., 2012). With the LIDEL model, we aimed to balance these concerns. The LIDEL model is driven with broadly available litter chemistry data and includes dynamic microbial CUE, but maintains a relatively simple first-order structure by not linking microbial biomass directly to decomposition rates (Fig. 1).

However, the results from our hierarchical Bayesian analysis, assimilating data from Soong et al. (2015) as well as from the literature (Adair et al., 2008; Parton et al., 2007), clarified several areas in need of targeted experimental focus to move the LIDEL model forward as a general model of litter decomposition. For example, as discussed above, the soluble fraction of plant litter is conceptually well defined as an important contributor to DOC generation with leaching. However, this litter fraction is difficult to measure in a way that links to its ecological function and variability (Soong et al., 2014). Measurement of the soluble litter fraction using hot water extraction was more variable than measurement by mass-difference (Fig. 5A). Both estimates were variable relative to the posterior distributions of the true soluble litter fractions (Fig. 5B), making it difficult to determine whether one measurement or the other is a more consistent approach. In addition, it is uncertain how laboratory measurements of soluble litter fractions relate to the dynamics of this material in a more complex field environment, where exposure to water and microorganisms are also more variable. Our assumption of constant exposure to water during leaching events did not allow us to explore this dynamic, and is an important area for further model development.

The relationship between measures of soluble plant litter fractions and variability in the true plant litter soluble fractions, both within and across litter types and in the context of varying decomposition environments, need to be better understood. This could be accomplished through comparative measures of a variety of litters from a variety of sources, using multiple extraction techniques. These types of data could help improve LIDEL model predictions of litter-derived DOC. LIDEL model formulations using higher DOC generation efficiency from the soluble litter pool (models 2 and 4, Fig. 6-2A and 4A) more accurately simulated high DOC generation, but were also more variable in their predictions, likely due to the broad priors used to initialize the soluble litter fraction.

As another example, in the initial conditions analysis we estimated an unknown model parameter: f_{DOC}, or the fraction of soluble plant litter that avoids microbial processes and is immediately released from plant litter through leaching alone. A large fraction of DOM can be leached directly from fresh litter (Don and Kalbitz, 2005), and numerous studies have observed large portions of DOM emerging from leaf litter early in decomposition (Cleveland et al., 2004; Magill and Aber, 2000). This is an important component to model accurately, as it may contribute to mineral-associated SOM formation in early litter decomposition (Cotrufo et al., 2015; Haddix et al., 2016). This soluble material will also likely have different characteristics (C:N, timing of generation) than DOM generated through the microbial pathways, which may affect its dynamics as it moves into the soil profile. In our initial conditions analysis we estimated initial f_{DOC} using the cumulative DOC measured from day 0 – day 10 of the Soong et al. (2015) experiment. The data poorly informed the parameter posterior distribution, yielding the broadest 95% BCI width of all of the parameters in this component of the analysis (Table 5). We also observed that the use of this parameter's posterior distribution to as a prior to initialize the pine DOC pool (in the temporal dynamic Bayesian analysis) resulted in initial DOC estimates that were higher than DOC cumulatively reached in the Soong et al. (2015) experiment. We therefore added a 'structural protection' coefficient (0.4) for pine initial DOC, based on the assumption that needle litters have a molecular structure that allows for a greater protection of plant soluble C in early decomposition (Don and Kalbitz, 2005). Specific initial f_{DOC} parameters may need to be determined to improve model estimates of litter-specific variability in this product of litter decomposition. This is also a value that may vary depending on the quantity and timing of the initial leaching event, which we could not examine given the limitations of Soong et al. (2015) experimental methods. Cumulatively, these results suggest the need to better understand factors that determine the quantity of litter organic matter that escapes microbial processing with leaching events early in litter decomposition.

The LIDEL model provides a theoretical structure to connect litter chemistry and microbial processes to the generation of microbial-derived soluble *versus* structural material (Moorhead et al., 2013; Sinsabaugh et al., 2013). However, from this analysis there remains uncertainty in the internal dynamics of the model, particularly the rate of microbial biomass turnover and the subsequent fractionation between soluble *versus* structural microbial products. These uncertainties could be addressed with data evaluating the relative contribution of microbial-derived *versus* plant-derived DOC during litter decomposition (Simpson and Simpson, 2012). Furthermore, N control of microbial generation of DOC

versus microbial products can be simulated by the LIDEL model but was not a hypothesis we could explore given the available data. This is potentially an important consideration for stabilization of litter inputs in soils, as soluble *versus* structural microbial products from litter decomposition may contribute to different pathways of SOM formation (Cotrufo et al., 2015).

5. Conclusions

In this analysis we presented the LIDEL model, a new litter decomposition model that includes dynamic lignin and N controls on microbial CUE and simulates the partitioning of litter decomposition products to DOC with leaching, CO_2, microbial biomass, and microbial products. We determined that N limitation on processes that partition litter C during decomposition are better represented as occurring rapidly at a threshold available N value, and that DOC generation with leaching occurs more efficiently from the decay of soluble *versus* holocellulose litter C. By simulating the generation of these dissolved and particulate litter C products using widely available litter chemistry data, the LIDEL model is a generalizable approach to litter decomposition that connects to important pathways of SOM formation (Cotrufo et al., 2015), that can thus better represent litter-derived C inputs to processed-based SOM models (Ahrens et al., 2015; Schmidt et al., 2011). We used hierarchical Bayesian methods to estimate LIDEL model parameters using experimental and literature-derived data, both for initial LIDEL conditions as well as parameters that drive LIDEL temporal dynamics. Some parameters had broader posterior distributions than others, due to variability in the measured data as well as the strength of the linkage between measurements and conceptually-defined LIDEL model pools. The LIDEL model provides a robust theoretical structure to connect litter chemistry to microbial processes and the partitioning of litter C during decomposition. However, additional data resolving the connection between measures of leaf soluble fractions and the conceptual dynamics of this modeled pool, as well as microbial-*versus* plant-derived DOC generation with leaching, are needed to better inform model parameters and reduce variability in model simulations.

Acknowledgements:

Funding for this research was generously provided by Shell Global Solutions (US), Inc., NSF DEB #0918482, NSF DEB #1145200, NSF-GRFP, NSF RET- Kathleen Guilbert, NSF DEB #1256754, US Department of Agriculture (USDA) cooperative research projects (Grants 58-5402-4-001 and 59-1902-4-00), USDA Ultraviolet-B (Grant 2014-34263-22038), USDA National Institute of Food and Agriculture (Grant 2015-67003-23456), and Colorado State University NSF OPUS Project (NSF DEB #1256754). We thank Susan Lutz for her assistance with graphics, as well as Katherine Renwick and Nathan Galloway for their feedback on the Bayesian analysis. We are grateful to two anonymous reviewers for providing suggestions and guidance for improving this manuscript.

Appendix A. Supplementary data

Supplementary data related to this article can be found at http://dx.doi.org/10.1016/j.soilbio.2016.06.007.

References

Adair, E.C., Parton, W.J., Del Grosso, S.J., Silver, W.L., Harmon, M.E., Hall, S.A., Burke, I.C., Hart, S.C., 2008. Simple three-pool model accurately describes patterns of long-term litter decomposition in diverse climates. Glob. Change Biol. 14, 2636–2660. http://dx.doi.org/10.1111/j.1365-2486.2008.01674.x.

Aerts, R., 1997. Climate, leaf litter chemistry and leaf litter decomposition in terrestrial ecosystems: a triangular relationship. Oikos 79, 439–449. http://dx.doi.org/10.2307/3546886.

Ahrens, B., Braakhekke, M.C., Guggenberger, G., Schrumpf, M., Reichstein, M., 2015. Contribution of sorption, DOC transport and microbial interactions to the 14C age of a soil organic carbon profile: insights from a calibrated process model. Soil Biol. Biochem. 88, 390–402. http://dx.doi.org/10.1016/j.soilbio.2015.06.008.

Ahrens, B., Reichstein, M., Borken, W., Muhr, J., Trumbore, S.E., Wutzler, T., 2014. Bayesian calibration of a soil organic carbon model using Δ14C measurements of soil organic carbon and heterotrophic respiration as joint constraints. Biogeosciences 11, 2147–2168. http://dx.doi.org/10.5194/bg-11-2147-2014.

Berliner, L., 1996. Hierarchical Bayesian time series models. In: Hanson, K.M., Silver, R.N. (Eds.), Maximum Entropy and Bayesian Methods. Fundamental Theories of Physics. Springer, New York, NY, pp. 15–22.

Braakhekke, M.C., Beer, C., Schrumpf, M., Ekici, A., Ahrens, B., Hoosbeek, M.R., Kruijt, B., Kabat, P., Reichstein, M., 2014. The use of radiocarbon to constrain current and future soil organic matter turnover and transport in a temperate forest. J. Geophys. Res. Biogeosci. 119, 372–391. http://dx.doi.org/10.1002/2013JG002420.

Braakhekke, M.C., Wutzler, T., Beer, C., Kattge, J., Schrumpf, M., Ahrens, B., Schöning, I., Hoosbeek, M.R., Kruijt, B., 2013. Modeling the vertical soil organic matter profile using Bayesian parameter estimation. Biogeosciences 10, 399–420.

Campbell, E.E., Paustian, K., 2015. Current developments in soil organic matter modeling and the expansion of model applications: a review. Environ. Res. Lett. 10, 123004. http://dx.doi.org/10.1088/1748-9326/10/12/123004.

Clark, J.S., 2007. 9.6 Bayesian state space models. In: Models for Ecological Data, an Introduction. Princeton University Press, Princeton, NJ, pp. 272–282.

Cleveland, C.C., Neff, J.C., Townsend, A.R., Hood, E., 2004. Composition, dynamics, and fate of leached dissolved organic matter in terrestrial ecosystems: results from a decomposition experiment. Ecosystems 7, 175–285. http://dx.doi.org/10.1007/s10021-003-0236-7.

Cotrufo, M.F., Soong, J.L., Horton, A.J., Campbell, E.E., Haddix, M.L., Wall, D.H., Parton, W.J., 2015. Formation of soil organic matter via biochemical and physical pathways of litter mass loss. Nat. Geosci. 8, 776–779. http://dx.doi.org/10.1038/ngeo2520.

Cotrufo, M.F., Wallenstein, M.D., Boot, C.M., Denef, K., Paul, E., 2013. The microbial efficiency-matrix stabilization (MEMS) framework integrates plant litter decomposition with soil organic matter stabilization: do labile plant inputs form stable soil organic matter? Glob. Change Biol. 19, 988–995. http://dx.doi.org/10.1111/gcb.12113.

Davidson, E.A., Savage, K.E., Finzi, A.C., 2014. A big-microsite framework for soil carbon modeling. Glob. Change Biol. 20, 3610–3620. http://dx.doi.org/10.1111/gcb.12718.

Del Grosso, S.J., Ogle, S.M., Parton, W.J., Breidt, F.J., 2010. Estimating uncertainty in N2O emissions from U.S. cropland soils. Glob. Biogeochem. Cycles 24, GB1009. http://dx.doi.org/10.1029/2009GB003544.

Don, A., Kalbitz, K., 2005. Amounts and degradability of dissolved organic carbon from foliar litter at different decomposition stages. Soil Biol. Biochem. 37, 2171–2179. http://dx.doi.org/10.1016/j.soilbio.2005.03.019.

Elliott, E.T., Paustian, K., Frey, S.D., 1996. Modeling the measurable or measuring the modelable: a hierarchical approach to isolating meaningful soil organic matter fractionations. In: Powlson, D.S., Smith, P., Smith, J.U. (Eds.), Evaluation of Soil Organic Matter Models, NATO ASI Series. Springer Berlin Heidelberg, pp. 161–179.

Frey, S.D., Lee, J., Melillo, J.M., Six, J., 2013. The temperature response of soil microbial efficiency and its feedback to climate. Nat. Clim. Change 3, 395–398. http://dx.doi.org/10.1038/nclimate1796.

Fujita, Y., Witte, J.-P.M., van Bodegom, P.M., 2014. Incorporating microbial ecology concepts into global soil mineralization models to improve predictions of carbon and nitrogen fluxes. Glob. Biogeochem. Cycles 28. http://dx.doi.org/10.1002/2013GB004595, 2013GB004595.

Gelman, A., Rubin, D.B., 1992. Inference from iterative simulation using multiple sequences. Stat. Sci. 7, 457–472. http://dx.doi.org/10.1214/ss/1177011136.

Geremia, C., White, P.J., Hoeting, J.A., Wallen, R.L., Watson, F.G.R., Blanton, D., Hobbs, N.T., 2014. Integrating population- and individual-level information in a movement model of Yellowstone bison. Ecol. Appl. 24, 346–362. http://dx.doi.org/10.1890/13-0137.1.

Geweke, J., 1992. Evaluating the accuracy of sampling-based approaches to calculating posterior moments. In: Bernado, J.M., Berger, J.O., Dawid, A.P., Smith, A.F.M. (Eds.), Bayesian Statistics 4. Clarendon Press, Oxford, UK.

Haddix, M.L., Paul, E.A., Cotrufo, M.F., 2016. Dual, differential isotope labeling shows the preferential movement of labile plant constituents into mineral-bonded soil organic matter. Glob. Change Biol. http://dx.doi.org/10.1111/gcb.13237.

Hararuk, O., Luo, Y., 2014. Improvement of global litter turnover rate predictions using a Bayesian MCMC approach. Ecosphere 5, 1–13.

Herman, J., Moorhead, D., Berg, B., 2008. The relationship between rates of lignin and cellulose decay in aboveground forest litter. Soil Biol. Biochem. 40, 2620–2626. http://dx.doi.org/10.1016/j.soilbio.2008.07.003.

Hobbs, N.T., Hooten, M.B., 2015. Simple Bayesian models. In: Bayesian Models: a Statistical Primer for Ecologists. Princeton University Press, Princeton, NJ, pp. 79–106.

Houghton, R.A., 2007. Balancing the global carbon budget. Annu. Rev. Earth Planet. Sci. 35, 313–347. http://dx.doi.org/10.1146/annurev.earth.35.031306.140057.

Ingwersen, J., Poll, C., Streck, T., Kandeler, E., 2008. Micro-scale modelling of carbon turnover driven by microbial succession at a biogeochemical interface. Soil Biol.

Biochem. 40, 864–878. http://dx.doi.org/10.1016/j.soilbio.2007.10.018.
Klotzbücher, T., Kaiser, K., Guggenberger, G., Gatzek, C., Kalbitz, K., 2011. A new conceptual model for the fate of lignin in decomposing plant litter. Ecology 92, 1052–1062. http://dx.doi.org/10.1890/10-1307.1.
Lekkerkerk, L., Lundkvist, H., Ågren, G.I., Ekbohm, G., Bosatta, E., 1990. Decomposition of heterogeneous substrates; an experimental investigation of a hypothesis on substrate and microbial properties. Soil Biol. Biochem. 22, 161–167. http://dx.doi.org/10.1016/0038-0717(90)90081-A.
Levins, R., 1966. The strategy of model building in population biology. Am. Sci. 54, 421–431.
Magill, A.H., Aber, J.D., 2000. Dissolved organic carbon and nitrogen relationships in forest litter as affected by nitrogen deposition. Soil Biol. Biochem. 32, 603–613. http://dx.doi.org/10.1016/S0038-0717(99)00187-X.
Manzoni, S., Jackson, R., Trofymow, J., Porporato, A., 2008. The global stoichiometry of litter nitrogen mineralization. Science 321, 684–686. http://dx.doi.org/10.1126/science.1159792.
Manzoni, S., Piñeiro, G., Jackson, R.B., Jobbágy, E.G., Kim, J.H., Porporato, A., 2012. Analytical models of soil and litter decomposition: solutions for mass loss and time-dependent decay rates. Soil Biol. Biochem. 50, 66–76. http://dx.doi.org/10.1016/j.soilbio.2012.02.029.
Miltner, A., Bombach, P., Schmidt-Brücken, B., Kästner, M., 2011. SOM genesis: microbial biomass as a significant source. Biogeochemistry 111, 41–55. http://dx.doi.org/10.1007/s10533-011-9658-z.
Moorhead, D.L., Lashermes, G., Sinsabaugh, R.L., Weintraub, M.N., 2013. Calculating co-metabolic costs of lignin decay and their impacts on carbon use efficiency. Soil Biol. Biochem. 66, 17–19.
Moorhead, D.L., Sinsabaugh, R.L., 2006. A theoretical model of litter decay and microbial interaction. Ecol. Monogr. 76, 151–174. http://dx.doi.org/10.1890/0012-9615(2006)076[0151:ATMOLD]2.0.CO;2.
Ogle, K., Pendall, E., 2015. Isotope partitioning of soil respiration: a Bayesian solution to accommodate multiple sources of variability. J. Geophys. Res. Biogeosci. 120, 221–236. http://dx.doi.org/10.1002/2014JG002794.
Ogle, S.M., Breidt, F.J., Easter, M., Williams, S., Killian, K., Paustian, K., 2010. Scale and uncertainty in modeled soil organic carbon stock changes for US croplands using a process-based model. Glob. Change Biol. 16, 810–822. http://dx.doi.org/10.1111/j.1365-2486.2009.01951.x.
Ogle, S.M., Breidt, F.J., Easter, M., Williams, S., Paustian, K., 2007. An empirically based approach for estimating uncertainty associated with modelling carbon sequestration in soils. Ecol. Model. 205, 453–463. http://dx.doi.org/10.1016/j.ecolmodel.2007.03.007.
Ota, M., Nagai, H., Koarashi, J., 2013. Root and dissolved organic carbon controls on subsurface soil carbon dynamics: a model approach. J. Geophys. Res. Biogeosci. 118, 1646–1659. http://dx.doi.org/10.1002/2013JG002379.
Pagel, H., Ingwersen, J., Poll, C., Kandeler, E., Streck, T., 2014. Micro-scale modeling of pesticide degradation coupled to carbon turnover in the detritusphere: model description and sensitivity analysis. Biogeochemistry 117, 185–204. http://dx.doi.org/10.1007/s10533-013-9851-3.
Parton, W.J., Stewart, J.W.B., Cole, C.V., 1988. Dynamics of C, N, P and S in grassland soils - a model. Biogeochemistry 5, 109–131. http://dx.doi.org/10.1007/BF02180320.
Parton, W., Silver, W.L., Burke, I.C., Grassens, L., Harmon, M.E., Currie, W.S., King, J.Y., Adair, E.C., Brandt, L.A., Hart, S.C., Fasth, B., 2007. Global-scale similarities in nitrogen release patterns during long-term decomposition. Science 315, 361–364. http://dx.doi.org/10.1126/science.1134853.
Paustian, K., Schnurer, J., 1987. Fungal growth-response to carbon and nitrogen limitation - a theoretical-model. Soil Biol. Biochem. 19, 613–620. http://dx.doi.org/10.1016/0038-0717(87)90107-6.
Plummer, M., Best, N., Cowles, K., Vines, K., 2006. CODA: convergence diagnosis and output analysis for MCMC. R. News 6, 7–11.
Prescott, C.E., 2010. Litter decomposition: what controls it and how can we alter it to sequester more carbon in forest soils? Biogeochemistry 101, 133–149. http://dx.doi.org/10.1007/s10533-010-9439-0.
Preston, C.M., Nault,, J.R., Trofymow, J.A., 2009. Chemical changes during 6 years of decomposition of 11 litters in some Canadian forest sites. Part 2. 13C abundance, solid-state 13C NMR spectroscopy and the meaning of "Lignin." Ecosystems 12, 1078–1102. http://dx.doi.org/10.1007/s10021-009-9267-z.
Qualls, R.G., Haines, B.L., Swank, W.T., 1991. Fluxes of dissolved organic nutrients and humic substances in a deciduous forest. Ecology 72, 254–266. http://dx.doi.org/10.2307/1938919.
R Core Team, 2014. R: a Language and Environment for Statistical Computing. R Foundation for Statistical Computing, Vienna, Austria.
Rumpel, C., Kögel-Knabner, I., 2010. Deep soil organic matter—a key but poorly understood component of terrestrial C cycle. Plant Soil 338, 143–158. http://dx.doi.org/10.1007/s11104-010-0391-5.
Schmidt, M.W.I., Torn, M.S., Abiven, S., Dittmar, T., Guggenberger, G., Janssens, I.A., Kleber, M., Kögel-Knabner, I., Lehmann, J., Manning, D.A.C., Nannipieri, P., Rasse, D.P., Weiner, S., Trumbore, S.E., 2011. Persistence of soil organic matter as an ecosystem property. Nature 478, 49–56. http://dx.doi.org/10.1038/nature10386.
Simpson, M., Simpson, A., 2012. The chemical ecology of soil organic matter molecular constituents. J. Chem. Ecol. 38, 768–784. http://dx.doi.org/10.1007/s10886-012-0122-x.
Sinsabaugh, R.L., Manzoni, S., Moorhead, D.L., Richter, A., 2013. Carbon use efficiency of microbial communities: stoichiometry, methodology and modelling. Ecol. Lett. 16, 930–939. http://dx.doi.org/10.1111/ele.12113.
Smolander, A., Kitunen, V., 2002. Soil microbial activities and characteristics of dissolved organic C and N in relation to tree species. Soil Biol. Biochem. 34, 651–660. http://dx.doi.org/10.1016/S0038-0717(01)00227-9.
Soetaert, K., Petzoldt, T., Setzer, R.W., 2010. Solving differential equations in R: package deSolve. J. Stat. Softw. 33, 1–25.
Soong, J.L., Calderón, F.J., Betzen, J., Cotrufo, M.F., 2014. Quantification and FTIR characterization of dissolved organic carbon and total dissolved nitrogen leached from litter: a comparison of methods across litter types. Plant Soil 385, 125–137. http://dx.doi.org/10.1007/s11104-014-2232-4.
Soong, J.L., Parton, W.J., Calderon, F., Campbell, E.E., Cotrufo, M.F., 2015. A new conceptual model on the fate and controls of fresh and pyrolized plant litter decomposition. Biogeochemistry 124, 27–44. http://dx.doi.org/10.1007/s10533-015-0079-2.
Stockmann, U., Adams, M.A., Crawford, J.W., Field, D.J., Henakaarchchi, N., Jenkins, M., Minasny, B., McBratney, A.B., Courcelles, V. de R. de, Singh, K., Wheeler, I., Abbott, L., Angers, D.A., Baldock, J., Bird, M., Brookes, P.C., Chenu, C., Jastrow, J.D., Lal, R., Lehmann, J., O'Donnell, A.G., Parton, W.J., Whitehead, D., Zimmermann, M., 2013. The knowns, known unknowns and unknowns of sequestration of soil organic carbon. Agric. Ecosyst. Environ. 164, 80–99. http://dx.doi.org/10.1016/j.agee.2012.10.001.
Swift, M.J., Heal, O.W., Anderson, J.M., 1979. Decomposition in Terrestrial Ecosystems. University of California Press.
Tipping, E., Chamberlain, P., Fröberg, M., Hanson, P., Jardine, P., 2012. Simulation of carbon cycling, including dissolved organic carbon transport, in forest soil locally enriched with 14C. Biogeochemistry 108, 91–107. http://dx.doi.org/10.1007/s10533-011-9575-1.
Treseder, K.K., Balser, T.C., Bradford, M.A., Brodie, E.L., Dubinsky, E.A., Eviner, V.T., Hofmockel, K.S., Lennon, J.T., Levine, U.Y., MacGregor, B.J., Pett-Ridge, J., Waldrop, M.P., 2012. Integrating microbial ecology into ecosystem models: challenges and priorities. Biogeochemistry 109, 7–18. http://dx.doi.org/10.1007/s10533-011-9636-5.
Tuomi, M., Vanhala, P., Karhu, K., Fritze, H., Liski, J., 2008. Heterotrophic soil respiration—Comparison of different models describing its temperature dependence. Ecol. Model. 211, 182–190. http://dx.doi.org/10.1016/j.ecolmodel.2007.09.003.
Van Soest, P.J., Wine, R.H., 1968. Determination of lignin and cellulose in acid-detergent fiber with permanganate. J. Assoc. Off. Anal. Chem. 51, 780–785.
Wang, Y.P., Chen, B.C., Wieder, W.R., Leite, M., Medlyn, B.E., Rasmussen, M., Smith, M.J., Agusto, F.B., Hoffman, F., Luo, Y.Q., 2014. Oscillatory behavior of two nonlinear microbial models of soil carbon decomposition. Biogeosciences 11, 1817–1831. http://dx.doi.org/10.5194/bg-11-1817-2014.
Wieder, W.R., Bonan, G.B., Allison, S.D., 2013. Global soil carbon projections are improved by modelling microbial processes. Nat. Clim. Change 3, 909–912. http://dx.doi.org/10.1038/nclimate1951.
Wieder, W.R., Grandy, A.S., Kallenbach, C.M., Bonan, G.B., 2014. Integrating microbial physiology and physiochemical principles in soils with the MIcrobial-MIneral Carbon Stabilization (MIMICS) model. Biogeosci. Discuss. 11, 1147–1185. http://dx.doi.org/10.5194/bgd-11-1147-2014.
Woo, D.K., Quijano, J.C., Kumar, P., Chaoka, S., Bernacchi, C.J., 2014. Threshold dynamics in soil carbon storage for bioenergy crops. Environ. Sci. Technol. 48, 12090–12098. http://dx.doi.org/10.1021/es5023762.
Xu, X., Thornton, P.E., Post, W.M., 2013. A global analysis of soil microbial biomass carbon, nitrogen and phosphorus in terrestrial ecosystems. Glob. Ecol. Biogeogr. 22, 737–749. http://dx.doi.org/10.1111/geb.12029.